Nanotechnology for Environmental Engineering (2023) 8:413–423
https://doi.org/10.1007/s41204-022-00297-3

ORIGINAL PAPER

Microwave-assisted green synthesis of SnO_2 nanoparticles and their photocatalytic degradation and antibacterial activities

M. Manimaran[1] · A. Muthuvel[2] · Nejla Mahjoub Said[3,4]

Received: 13 April 2021 / Accepted: 2 November 2022 / Published online: 17 November 2022

Abstract

The development of nanoparticles based on plant material has many advantages over traditional physicochemical methods and has many applications in industrial and medical. In the present investigation, SnO_2 nanoparticles based on aqueous leaf extract of *Solanum nigrum* were prepared through the microwave-assisted method. The synthesized nanoparticles were characterized using by UV–visible, HR-TEM with SAED, XRD, ZE, DLS, BET surface area, FT-IR and PL analysis. XRD analysis demonstrated characteristic peaks in the crystallization planes (100), (101), (200), (211), (002), (310), (301), (202) and (222) of the SnO_2 nanoparticles. The HR-TEM revealed the formation of spherical morphology with a mean diameter of 18 nm. DLS supported that the average particle size 45 nm and zeta potential showed − 24.56 mV with a single peak. The presence of a protein shell outside the nanoparticles was confirmed by FT-IR analysis, which supports in their stabilization. The photocatalyst activities of the green-synthesized SnO_2 nanoparticles have been investigated by degradation of Evan blue (EB) dye under sunlight irradiation. Furthermore, disc diffusion was used to evaluate the bacterial activities of the synthesized nanoparticles against human pathogens and standard strains of gram-positive and gram-negative bacteria. SnO_2 nanoparticles exposed higher antibacterial activities against *E. coli* and lesser antibacterial activity against *B. subtillis* at higher concentration. Thus, plant-based nanoparticle synthesis could play a critical role in destroying bacterial pathogens and water purification.

Keywords SnO_2 · Microwave · *Solanum nigrum* · BET surface · Photocatalyst · Antibacterial

Abbreviations

SnO_2	Tin oxide
ZnO	Zinc oxide
CuO	Copper oxide
CeO_2	Cerium oxide
UV–Vis	UV–visible spectroscopy
HR-TEM	High-resolution transmission electron microscopy
SAED	Selected area electron diffraction
XRD	X-ray diffraction analysis
ZE	Zeta potential
DLS	Dynamic light scattering
BET	Brunauer–Emmett–Teller
FT-IR	Fourier-transform infrared spectroscopy
PL	Photoluminescence
nm	Nanometre
mV	Millivolt
eV	Electron volt
EB	Evan blue
mL	Millilitre
mg	Milligram
g	Gram
µg	Microgram
°C	Celsius
min	Minutes
h	Hour

✉ A. Muthuvel
phymuthu89@gmail.com

[1] Department of Chemistry, Paavendhar College of Arts and Science, Manivizhundan, Salem, Tamil Nadu 636102, India

[2] PG and Research Department of Physics, T.B.M.L. College (Affiliated to Bharathidasan University-Tiruchirappalli-620024), Porayar, Tamil Nadu 609307, India

[3] Department of Physics, College of Science, King Khalid University, Abha 61413, Saudi Arabia

[4] LGM, Preparatory Institute for Engineering Studies, University of Monastir, Monastir, Tunisia

Introduction

In recent years, one of the most environmentally sustainable approaches for preparing nanoparticles is the green synthesis approach. Many issues could be avoided if nanomaterials were synthesized using biosynthesis rather than chemical synthesis. The preparation process for the biosynthesis method does not use any toxic reagents [1]. Plant materials, micro-organisms, and enzymes are three types of materials widely used in the biosynthesis process [2]. Plant extract is one of them, and the simplest approach is to synthesize nanomaterials, which are low cost, abundant resource, and have easy operation requirements [3]. Plants are still used as a source of certain potent medications in many countries. This scientific advance is used all completed the world and their goods are also available on a more scale [4]. Plants have a high genetic diversity in terms of biomolecules and metabolites such as alkaloids, flavonoids, phenols, saponins, proteins, vitamins and coenzyme-based intermediates. Plant metabolites contain hydroxyl (OH), carboxylic acids (CO_2H) and amine (NH_2) functional groups, which react with metal ions to make them nanoscale [5]. In the biosynthesis of nanoparticles from plant extracts, may metals have been commonly used, such as gold, silver, zinc, copper and many others [6–9]. Recently, Nabil Al-Zaqri et al. [10] used *Wrightia tinctoria* leaf extract to biosynthesize zirconium oxide nanoparticles. Kora et al. [11] investigated catalytic dye degradation studies for various dyes and reported the effective preparation of palladium nanoparticles using *Anogeissus latifolia* leaf extract. Stannic oxide (SnO_2) is a stable, n-type semiconductor material with a band gap of ($E_g = 3.5$ eV) that has been generally used in photosensors, gas sensors, antistatic coatings, and photocatalysts [12]. SnO_2 nanoparticles have also been found to have possible biological applications as effective antibacterial and antioxidant agents, bioimaging probes, drug carriers, and cancer-curing cytotoxic agents [13]. Solgel [14], hydrothermal [15], chemical precipitation [16], solvothermal [17], sonochemical [18], combustion path [19], and microwave technique [20] have all been used to synthesize SnO_2 nanoparticles. In this study, attributed to its properties, we have provided an inexpensive and simple method for microwaves. Microwaves produce high power densities, allowing for more efficient output at lower costs. Microwave systems are more compact, requiring less space for equipment and production times, as well as cleaning and chemical costs, are reduced [21]. Microwave irradiation penetrates the sample better than traditional methods, resulting in a uniform temperature distribution between the surface and the bulk material as well as temperature stability during microwave processing and heating, resulting in the rapid production of SnO_2 nanoparticles [22]. For the preparation of SnO_2 nanoparticles, most investigators have identified the use of medicinal plants such as *Andrographis Paniculata*, *Punica Granatum*, *Catunaregam Spinosa*, *Calotropis gigantean*, *Camellia sinensis*, *Amaranthus tricolor* and *Indica* flower (Table 1). In the literature, ZnO [30], CuO [31] and CeO_2 [32] nanoparticles were synthesized using *Solanum nigrum* leaf extract. However, to the best of our knowledge, no reports on biosynthesis of SnO_2 nanoparticles using *Solanum nigrum* leaf extract were reported.

Solanum nigrum belongs to family of Solanaceae and commonly known as manathakkali in Tamil. *Solanum nigrum* leaves have been found to be medicinal uses and are used to treat lung diseases and ailments. Antibacterial, antioxidant, anti-genotoxic, anti-tumorigenic and anti-inflammatory effects of *Solanum nigrum* have been demonstrated. The leaves hold flavones, phenols, alkaloids, carbohydrates and aromatic compounds in great amounts [31]. These complexes are phytochemicals agents which are cause for the capping and stabilizing process of nanoparticles. Hence, the present work designs to synthesize SnO_2 nanoparticles using the microwave-assisted method (*Solanum nigrum* leaf extract; reducing agent). The optical, structural, morphological and luminescence properties of the synthesized nanoparticles were investigated. Furthermore, under sunlight irradiation, the prepared SnO_2 nanoparticles were undergoing Evan blue dye degradation and antibacterial activity.

Materials and methods

Materials

As oxidizers, analytical-grade $SnCl_2.2H_2O$ and Evan blue (EB) dye (Hi-Media India) were used. Both gran-positive and gram-negative bacteria including *B. subtilis* (*Bacillus subtilis)*, *S. aureus (Staphylococcus aureus) E. coli (Escherichia coli)* and *P. aeruginosa (Pseudomonas aeruginosa*)

Table 1 SnO_2 nanoparticles synthesized from different plant extracts

S. no.	Plant extract	Morphology	Crystallite size (nm)	References
1	*Andrographis Paniculata*	Nanoparticles	27.0	[23]
2	*Punica Granatum*	Nanoparticles	8.64	[24]
3	*Catunaregam Spinosa*	Nanoparticles	46.0	[25]
4	*Calotropis gigantea*	Nanoparticles	35.0	[26]
5	*Camellia sinensis*	Nanoparticles	16.1	[27]
6	*Amaranthus tricolor*	Nanoparticles	18.9	[28]
7	*Indica* flower	Nanoparticles	11.4	[29]

were bought from Institute of Microbial Technology, Chandigarh, India. As a solvent, Milli-Q (Millipore Elix, India) used double-distilled water during the reaction. Analytical-grade chemicals were used in all experiments.

Preparation of the leaf extract

We collected the *Solanum nigrum* leaves from Chidambaram, Tamil Nadu, India. To remove any contamination, we thoroughly washed the leaves with tap water and distilled water. During a week of air drying, the leaves were kept at room temperature. Through the support of a pestle and mortar, about 10 g of *Solanum nigrum* leaf powder was ground. Five grams of powder was mixed with 250 mL of distilled water in a 500-mL beaker and heated at 85 °C for 20 min. After cooling the extract to room temperature, muslin cloth and then Whatman filter paper No:1 were used to filter the mixture, which was then stored at 4 °C.

Biosynthesis of SnO_2 nanoparticles

In this study, SnO_2 nanoparticles were prepared by green synthesis, as in previous studies [23]. 10 mL of *Solanum nigrum* leaf extract added is dropwise with 100 mL of (1.25 g) aqueous stannous chloride solution. Additionally, the solution was homogenized with glass rods. The synthesis was carried out in a domestic microwave oven (800 W, 2.45 GHz). The above solution was put in a microwave oven and irradiated for 25 min in convection mode. In the end, the microwave oven sample was removed. After that, microwave-added organic impurities and unburned carbon were removed by calcining the SnO_2 nanoparticles at 600 °C for 6 h. A further analysis was conducted on white SnO_2 nanoparticles obtained as powders.

Characterization

In the present study, a JASCO V-670 spectrophotometer was used to record optical spectra in the range of 300–800 nm. The morphologies of the particles were confirmed using HR-TEM (PHILLIPS TECNAI G2 FEI 12). Dynamic light scattering (DLS) technique (Malvern Masettinds) is found on scattering of light by diffusion, which is measured by average size distribution, and the stability of nanoparticles was analysed by the zeta potential (ZE) analyser (Malvern Masettinds Nano instrument). The crystalline phase structures of the products were examined and studied by X-ray diffractometer (Riakgu Mini Flexell) operated at a 40 kV and current 30 mA with Cukα ($\lambda = 1.5406$ Å). A Perkin-Elmer LS 55 spectrophotometer was used to measure Photoluminescence (PL) at room temperature under emission spectra, with the measurements made at 340 nm wavelength.

Photocatalytic degradation activity

The green-synthesized SnO_2 nanoparticles were evaluated for photocatalyst degradation of the EB dye under sunlight irradiation. The UV light intensity was measured using YK-35 UV light meter at 7 $mWCm^{-2}$. At ambient temperature, the experiment was conducted between 12.00 and 2.00 pm. About 50 mL of EB dye (1.5×10^{-4}) solution containing 0.2 g of the catalyst suspensions was used for photocatalyst degradation. The catalyst mixture was stirred in the absence of light for 15 min and allowed to attain the equilibrium and then irradiated with a UV–Vis spectrometer at the range of 400 to 800 nm. After that, 3 mL of the catalyst solution was taken at periodic intervals (15 min), and the catalyst was recovered from the suspension by centrifugation. Absorbance $\lambda_{max} = 605$ nm for EB dye monitored under the UV–Vis spectrophotometer. The degradation percentage was measured by following expression [31]:

$$\eta = \frac{C_0 - C_t}{C_0} \times 100\% \quad (1)$$

where η is the percentage of degradation, C_0 is the beginning concentration of the EB dye, and C_t is the concentration after a time interval.

Antibacterial activity

The *Solanum nigrum* leaf extract and synthesized SnO_2 nanoparticles are tested for bacterial activities by the agar disc diffusion method against human pathogenic bacteria, viz., the gram-negative bacteria such an *E. coli* and *P. aeruginosa* and the gram-positive bacteria *B. subtilis* and *S. aureus*. Using a sterile cotton swab, each strain was swabbed uniformly onto the surface of the Mueller Hinton agar plate. The 5, 10, 25 and 50 µg/mL of the tested samples were added to the well at septic conditions. A positive control was an antibiotic disc containing Ciprofloxacin. After incubation for 24 h at 35 °C, the average zone of inhibition diameter was measured and tabulated.

Results and discussion

X-ray diffraction analysis

X-ray diffraction (XRD) was used to assess the crystallite size and phase purity of green-synthesized SnO_2 nanoparticles; the results are shown in Fig. 1. The majority of the perceptible Bragg's speaks with Miller indices (100), (101), (200), (211), (002), (310), (301), (202) and (222) can be recorded to the tetragonal structure of SnO_2

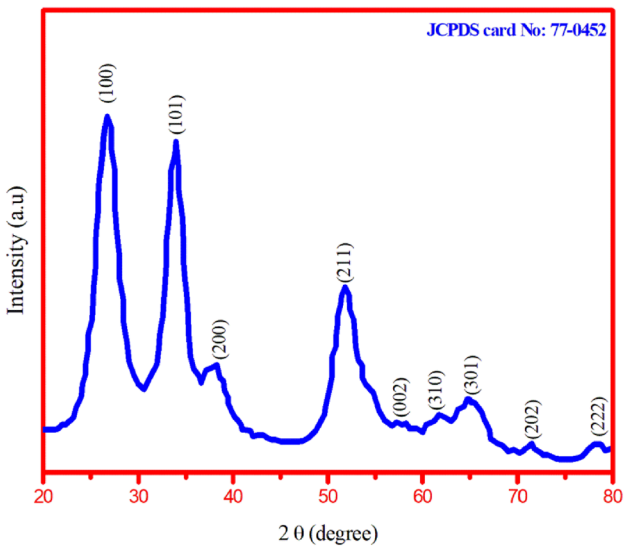

Fig. 1 XRD pattern of the synthesized SnO_2 nanoparticles

nanoparticles (JCPDS Card No: 77-0452) [26]. There were no other impurity peaks in the plots, indicating that the synthesized SnO_2 nanoparticles are of high phase purity. SnO_2 nanoparticles synthesized from *A. paniculata* leaf extract produced a similar result [23]. Scherer's equation [32] was used to measure the average crystallite size.

$$D = \frac{0.94\lambda}{\beta \cos\theta} \tag{2}$$

where λ is the wavelength coming from Cu-Kα (1.5406 Å), β is the full width of the diffraction peak at half maximum, θ is the angle of diffraction, and D is the size of the crystal. The average crystallite size of synthesized SnO_2 nanoparticles is found to be 5.13 nm, according to the calculations. As shown in Table 1, the size of the obtained crystallites (green synthesis of SnO_2 nanoparticles using microwave-assisted method) is much smaller than that of other leaf extracts used to synthesize SnO_2 nanoparticles. Different structural parameters of SnO_2 nanoparticles, such as lattice parameters, unit cell length, dislocation density, and micro-strain values, have been calculated using the following relationships, and the estimated values are tabulated in Table 2.

$$\frac{1}{d^2} = \frac{h^2 + k^2}{a^2} + \frac{l^2}{c^2} \tag{3}$$

$$V = a^2.c \tag{4}$$

$$\delta = \frac{1}{D^2} \tag{5}$$

$$\varepsilon = \frac{\beta \cos\theta}{4} \tag{6}$$

Table 2 shows that lower dislocation density and micro-strain improve the crystalline properties of synthesized SnO_2 nanoparticles.

HR-TEM analysis

The particles have a spherical morphology, as shown by HR-TEM images (Fig. 2a). Apart from that, studies of synthesized SnO_2 nanoparticles at 2 nm resolution reveal a 0.17 nm '*d*' space, indicating the crystalline existence of nanoparticles (Fig. 2b). The SAED pattern of synthesized SnO_2 nanoparticles is shown in Fig. 2c, with (100), (101), (200), (211), (002), (310), (301), (202) and (222) reflections corresponding to the rutile tetragonal structure, which matches the XRD results. Synthesized SnO_2 nanoparticles have an average size of 18 nm, as shown in Fig. 2d. According to the findings, the most porous nature favours the absorption of more dye molecules, which improves the photocatalyst's efficiency.

DLS and ZE analysis

The size distribution of SnO_2 nanoparticles synthesized in aqueous medium is represented in Fig. 3. DLS was used to measure it. The average particles size was 45 nm and Poly dispersity index of 0.247. The SnO_2 nanoparticles obtained in this study are monodisperse in nature. Figure 4 reveals that the zeta potential of synthesized SnO_2 nanoparticles was − 24.56 mV. The strong negative value confirms particles repulsion, and the negative value shows that nanoparticles are stable. Generally, ZE indicates how strongly neighbouring particles are repelled by electrostatic forces.

Table 2 The structural analysis of microwave-assisted green synthesis of SnO_2 nanoparticles

Sample	Average crystalline size (nm)	Lattice parameter (Å)		Unit cell volume (Å^3)	Micro-strain (ε)×10^4 lin^{-2} m^{-4}	Dislocation density (δ) 10^{14} lin/m^2
		$a=b$	c			
SnO_2	5.13	4.456	3.107	69.41	0.25647	3.0245

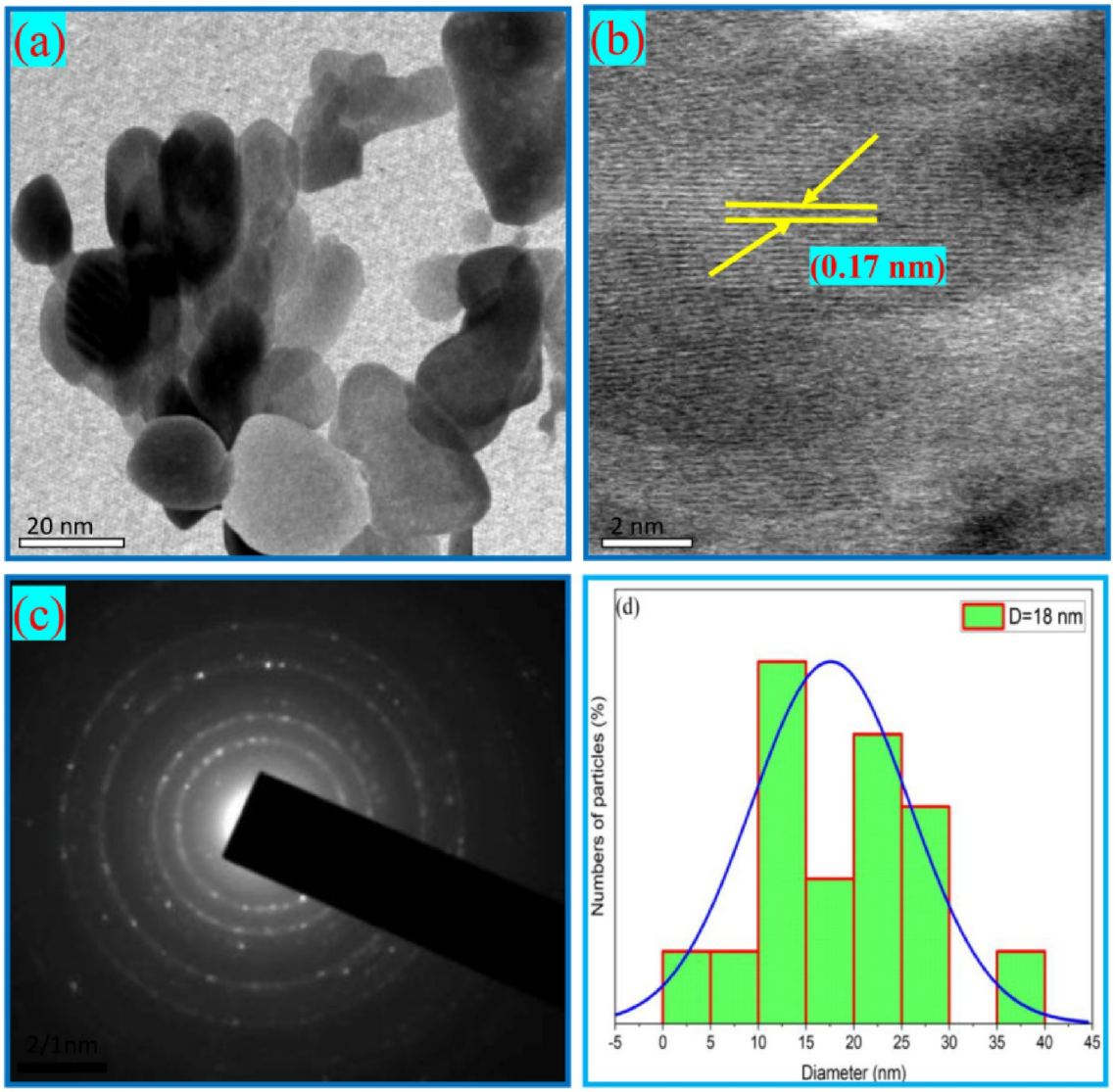

Fig. 2 (**a**) HR-TEM (**b**) lattice fringe (**c**) SAED (**d**) particles size of synthesized SnO_2 nanoparticles

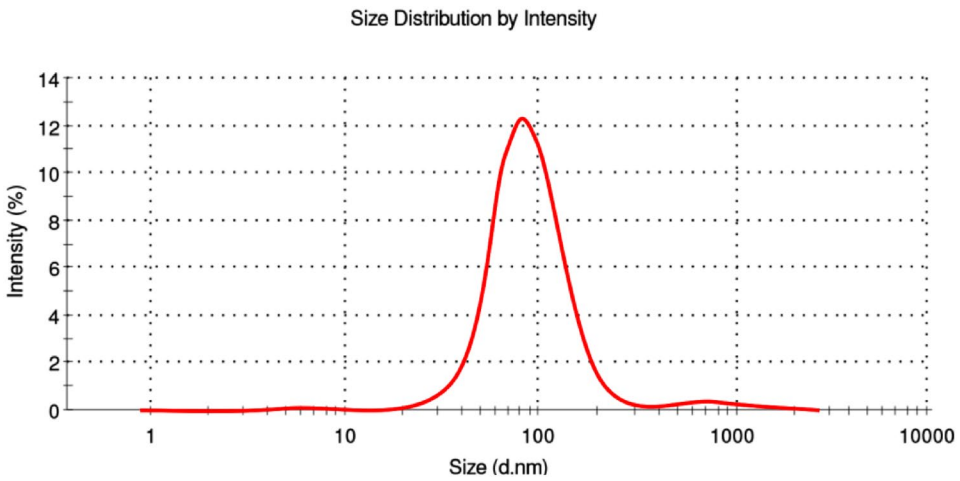

Fig. 3 DLS particle size analyzer of synthesized SnO_2 nanoparticles

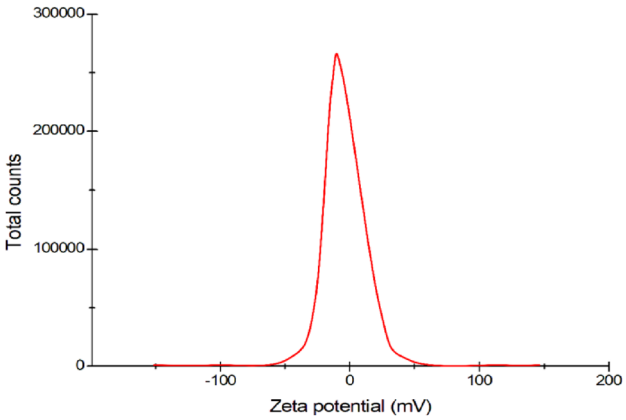

Fig. 4 Zeta potential analyzer of synthesized SnO_2 nanoparticles

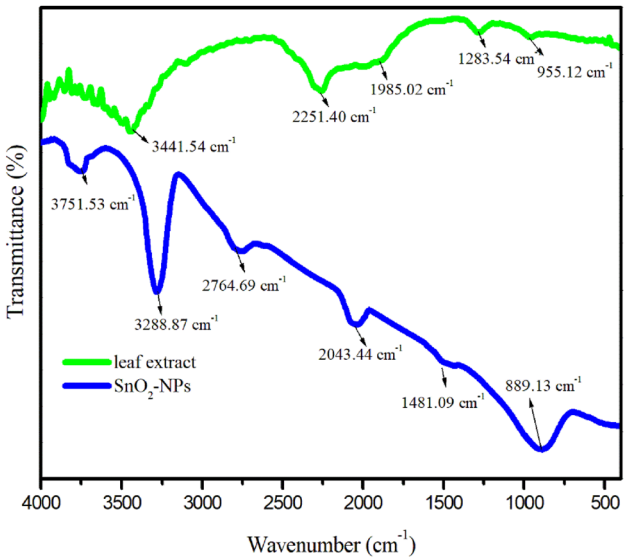

Fig. 5 FT-IR spectrum of the *Solanum nigrum* leaf extracts and synthesized SnO_2 nanoparticles

When OH^- ions adsorb on particles, their ZE values are negative, preventing particle aggregation and maintaining particle size. These results also established the monodispersed SnO_2 nanoparticles as proposed by Kumar et al. [33].

FT-IR analysis

Figure 5 displays the FT-IR spectrum of the green-synthesized SnO_2 nanoparticles, which were used to recognize the functional groups. The existence of major functional groups such as –OH stretching vibration (3441.54 cm^{-1}), C-H stretching vibration (2251.40 cm^{-1}), amine N–H group of protein (1985.02 cm^{-1}), cellulose (1283.54 cm^{-1}) and alkenes was observed in the *Solanum nigrum* leaf extract (955.12 cm^{-1}) [31]. FT-IR analysis confirmed the presence of carboxyl and amide groups in *Solanum nigrum* leaf extract. The bio-reduction of Tin ions into SnO_2 nanoparticles is carried out from these groups. The observed IR bands 3751.53 cm^{-1} and 3288.87 cm^{-1} correspond to the O–H stretching and O–H bending vibrations of water molecules [32] in the spectra provided by the study of green-synthesized SnO_2 nanoparticles (Fig. 5). The presence of an alcohol group has been indicated by the strong and broad peak observed at 2764.69 cm^{-1}, which corresponds to a (C–H) bond. Furthermore, the band at 2043.44 cm^{-1} is caused by the stretching of the C–H bond absorbed in the SnO_2 surface. Symmetric vibrations of the Sn–O bond were the lower intensity peak at 889.13 cm^{-1}. This finding is consistent with that of green-synthesized SnO_2 nanoparticles using with *Calotropis gigantea* [26].

UV–visible analysis

The UV–Vis spectrum of green-synthesized SnO_2 nanoparticles is shown in Fig. 6a. The presence of SnO_2 nanoparticles is indicated by the surface plasmon resonance peak at 344 nm exposed in Fig. 6a. The absorption peak of the synthesized SnO_2 nanoparticles is nearly the same as that of those recorded in the literature [25]. The bandgap energy of green-synthesized SnO_2 nanoparticles was determined using UV–visible spectroscopy data. Using the equation [31] as a reference,

$$\alpha h\nu = D\left(h\nu - E_g\right)^n \tag{7}$$

where A is photon energy ($h\nu$), Eg is band gap energy, and α and n are absorption coefficient. In green-synthesized SnO_2 nanoparticles, the measured band gap was 3.3 eV (Fig. 6b). In this case, it is likely that an intrinsic SnO_2 band gap absorption and electron transfer between the valence band and conduction band are responsible for this phenomenon [10]. The green-synthesized SnO_2 nanoparticles with minimum band gap energy could be used in photocatalytic activities.

PL analysis

A PL spectrum of green-synthesized SnO_2 nanoparticles with an excitation wavelength of 340 nm is shown in Fig. 7. The spectra of SnO_2 nanoparticles divided into three major peaks, i.e. 353, 402, and 421 nm, respectively. The spectra exhibit characteristic blue band edge emission at 353 nm, with a strong and intense peak, implying a deep level of emission to tin interstices of oxygen deficiencies and structural defects in SnO_2 nanoparticles. The emission at 402 nm has attributed to an electron transition induced by band gap defects such as oxygen vacancies [34]. The luminescence centre formed by such tin interstitials or dangling in the present SnO_2 nanoparticles could explain the peak at

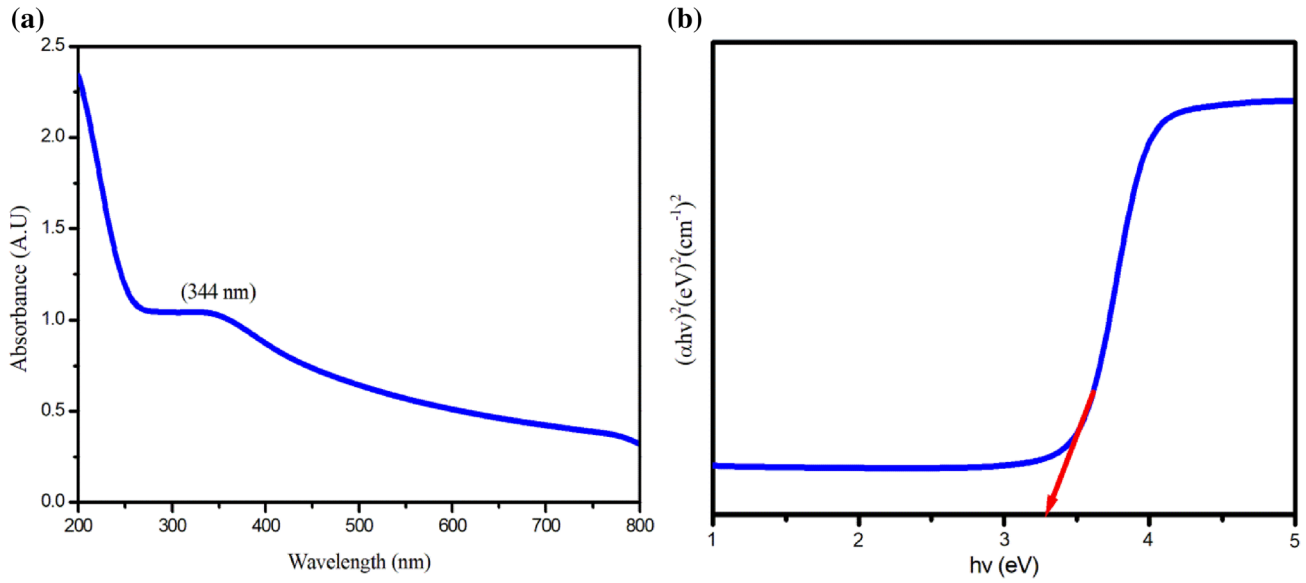

Fig. 6 (**a**) UV–Visible spectrum (**b**) bandgap energy of synthesized SnO_2 nanoparticles

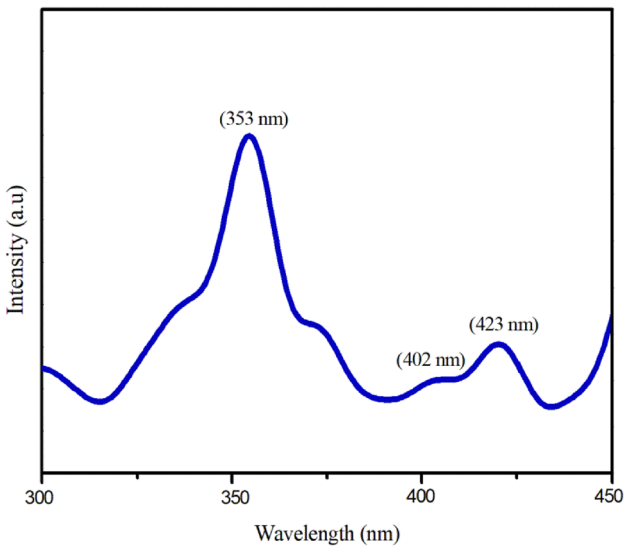

Fig. 7 PL spectra of the synthesized SnO_2 nanoparticles

421 nm [34]. SnO_2 nanoparticles have intrinsic defects such as oxygen vacancies, which serve as luminescent centres, which form defect levels highly located in the gap, trapping electrons from the valence band and contributing to luminescence. The PL emission properties of green-synthesized SnO_2 nanoparticles improve capabilities in photoluminescent and photocatalytic applications.

Specific surface area analysis

Surface area is critical for catalytic properties because it aids in reactant adsorption and desorption [35]. The porous existence of the synthesized SnO_2 nanoparticles has been investigated using unique surface area. The N_2 adsorption/desorption isotherms and pore size distribution plot of the synthesized SnO_2 nanoparticles are shown in Fig. 8a, b. According to the IUPC nomenclature, SnO_2 nanoparticles displaced type IV isotherm from desorption. The surface area of SnO_2 nanoparticles measured by BET is 153 m^2/g. According to these results, SnO_2 nanoparticles with a smaller particle size (19.71 nm) and a larger surface area will help improved photocatalyst properties.

Photocatalytic activities

The catalyst activity of green-synthesized SnO_2 nanoparticles was estimated from the degradation of EB dye kept under the sunlight irradiation. The photocatalytic degradation of EB dye is depicted in Fig. 9a. The time intervals used in this study ranged from 0 to 90 min. The degradation of EB dye was determined by measuring the absorbance at 607 nm (Fig. 9a). The dye catalytic activity of SnO_2 nanoparticles against EB dye was greater than 96% (Table 3). The degradation of EB dye as a photocatalyst has been attributed to its particle size, structure, band gap and crystallinity of the photocatalyst, surface area, and other factors [23]. The microwave-assisted green synthesis of SnO_2 nanoparticles using *Solanum nigrum* leaf extract was used as a catalyst because of its better bulkiness, purity, and high yield.

Kinetic studies

Under sunlight irradiation, the photocatalytic degradation of EB dye follows pseudo-first-order kinetics, as expressed by the equation [31]:

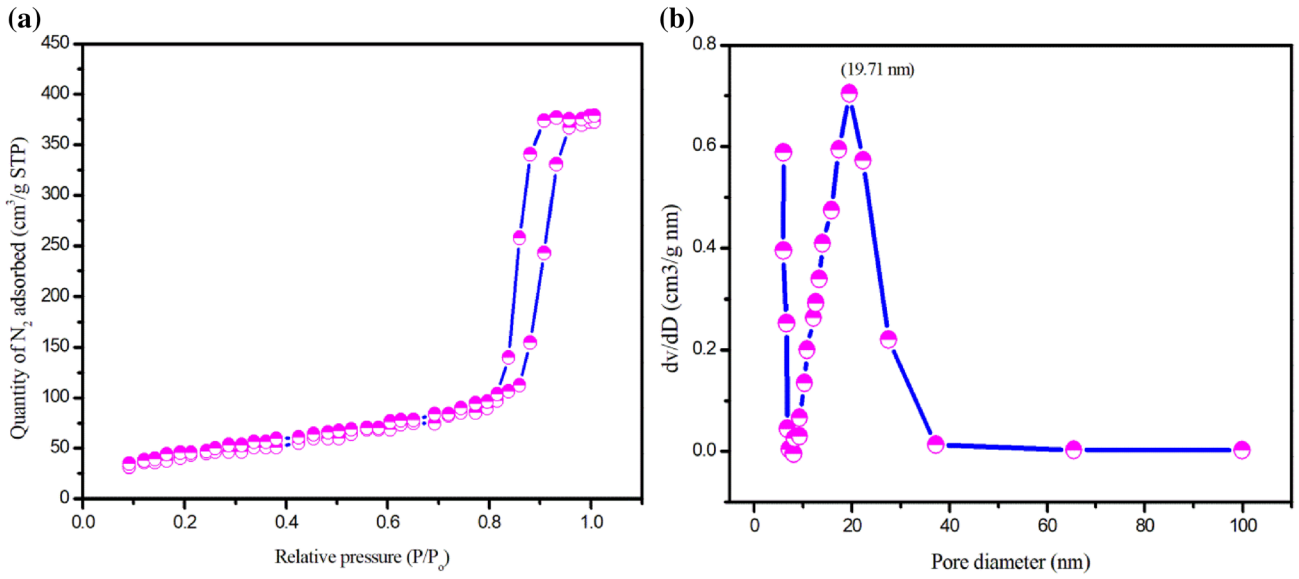

Fig. 8 (**a**) N_2 adsorption/desorption isotherms (**b**) BJH pore size distribution of synthesized SnO_2 nanoparticles

$$\text{In}\left(A_0/A_t\right) = -k_t \tag{8}$$

where k is the pseudo-first-order constant, At and Ao are the concentrations of EB dye at time t and 0, respectively, and t is the time in minutes. Figure 9b shows the kinetics of photocatalyst degradation of EB dye by synthesized SnO_2 nanoparticles. The rate constant for EB dye is 0.9754 min^{-1}, and the plot of In (C_o/C_t) as a function of irradiation time is 90 min. In addition, the fitting correlation coefficient (R^2) has been calculated to be 0.9946. The C_o/C_t value decreases as time increases, and vice versa, as well as the percentage of EB dye degradation increases with time.

Photocatalytic degradation mechanism of SnO_2 nanoparticles

$$SnO_2 + h\nu \rightarrow SnO_2(e^-_{CB} + h^+_{VB}) \tag{9}$$

$$SnO_2\left(h^+\right) + OH^- \rightarrow OH^0 \tag{10}$$

$$SnO_2\left(e^+\right) + O_2 \rightarrow O_2^{0-} \tag{11}$$

$$O_2^{0-} + H^+ \rightarrow HO^{2^0} \tag{12}$$

$$SnO_2(e^-) + H^+ + HO_{2^0} \rightarrow OH^0 + OH^- \tag{13}$$

$O_2{}^{0-} + HO_2{}^0 + OH^0$ or (h^+) + EB dye degradation product

From the reaction (Fig. 9c), the hydroxyl radical (^0OH) and superoxide radical $\left(O_2^0\right)$ are foremost dependable for the photocdegradation performance of the EB dye molecules [10].

Antibacterial activity

The bacterial activities of tested samples on gram-positive and gram-negative bacteria are shown in Table 4. Based on the table, the zone of inhibition increases as well as the concentrations of the sample. The leaf extract of *Solanum nigrum* showed the maximum inhibition zone at concentration of 50 µg/mL for *E. coli* (15 ± 0.3), *P. aeruginosa* (14 ± 0.2), *S. aureus* (13 ± 0.3) and *B. subtillis* (11 ± 0.1). The synthesized SnO_2 nanoparticles showed respectable bacterial activity against all tested micro-organisms as compared with *Solanum nigrum* leaf extract at a concentration of 50 µg/mL. The inhibition zone was observed against *E. coli* (25 ± 0.2), *P. aeruginosa* (23 ± 0.2), *S. aureus* (22 ± 0.1) and *B. subtillis* (21 ± 0.1). The particle size and surface area of a particulate drug delivery system are well known to play a significant role in their interactions with biological cells and the in vivo fate of the system. SnO_2 nanoparticles produce electronic effects due to their size and large surface area, and these effects can increase the nanoparticles' binding strength with bacteria. We hypothesised that the above mechanisms can account for SnO_2 nanoparticles excellent antibacterial activity when compared to *Solanum nigrum* leaf extract. At all concentrations, SnO_2 nanoparticles have a greater zone of inhibition against gram-negative bacteria than gram-positive bacteria. According to Muthuvel et al. [32], gram-positive bacteria were inhibited far more than gram-negative bacteria. In gram-negative bacteria, the outer membrane is solid

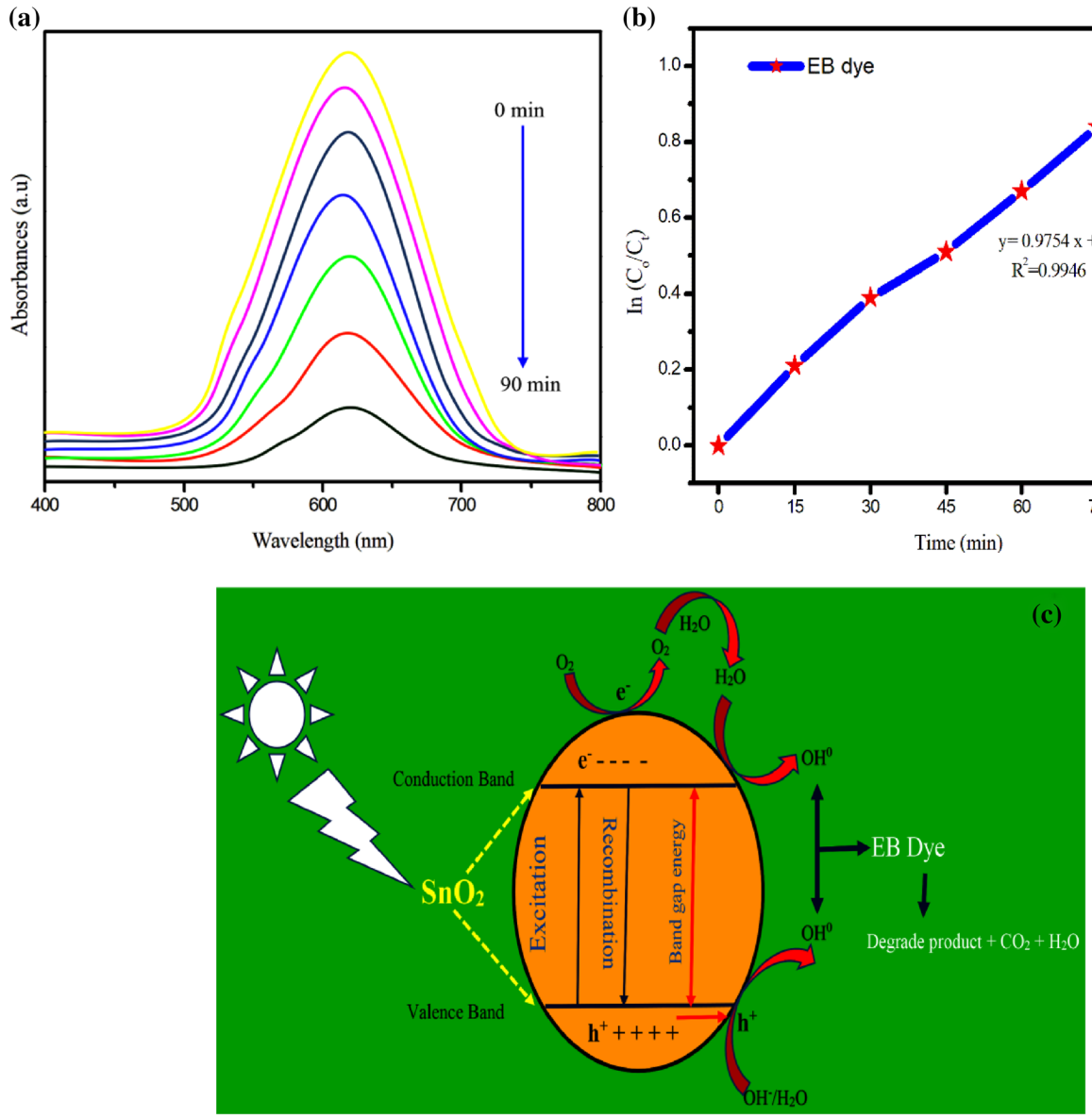

Fig. 9 (**a**) UV–Vis absorption spectra of EB dye with respect to irradiation time versus; (**b**) rate constant (*K*) and regression (R^2); (**c**) Mechanism for photodegradation of EB dye by synthesized SnO_2 nanoparticles

Table 3 Comparison of dye photocatalytic degradation rate

Catalyst	Prepared method	Dye	Reaction time (min)	Degradation rate (%)	References
SnO_2	Microwave-green synthesis	EB	90	96	This study
SnO_2	Hydrothermal	MB	120	90	[36]
SnO_2	Precipitation	MB	180	80	[37]
SnO_2	Co-precipitation	MB	60	60	[38]
SnO_2	Liquid phase deposition	MB	180	82	[39]
SnO_2	Biosynthesis	MB	180	80	[26]

Table 4 Antibacterial activity of *Solanum nigrum* leaf extract and synthesized SnO_2 nanoparticles against human pathogens

Bacteria's	Zone of inhabitations (mm)											
	5 µg/mL			10 µg/mL			25 µg/mL			50 µg/mL		
	Leaf	SnO_2	St	Leaf	SnO_2	St	Leaf	SnO_2	St	Leaf	SnO_2	St
B. subtillis	1 ± 0.3	5 ± 0.2	7 ± 0.1	3 ± 0.2	9 ± 0.2	12 ± 0.2	7 ± 0.2	14 ± 0.2	17 ± 0.2	11 ± 0.1	21 ± 0.1	25 ± 0.2
S. aureus	1 ± 0.1	4 ± 0.2	7 ± 0.4	4 ± 0.4	10 ± 0.4	14 ± 0.1	8 ± 0.2	15 ± 0.1	19 ± 0.4	13 ± 0.3	22 ± 0.1	25 ± 0.2
E. coli	2 ± 0.3	6 ± 0.5	10 ± 0.3	7 ± 0.2	12 ± 0.1	16 ± 0.2	12 ± 0.1	17 ± 0.1	21 ± 0.4	15 ± 0.3	25 ± 0.2	27 ± 0.1
P. aeruginosa	1 ± 0.4	5 ± 0.2	9 ± 0.2	6 ± 0.2	13 ± 0.3	15 ± 0.2	10 ± 0.2	15 ± 0.3	21 ± 0.1	14 ± 0.2	23 ± 0.2	26 ± 0.2

St standard

and hydrophobic. Based on these results, microwave-assisted green-synthesized of SnO_2 nanoparticles using *Solanum nigrum* leaf extract could be effective against gram-negative bacteria such as *E. coli*. This may be attributed to the presence of more phenols, flavonoids and saponins compounds and specific secondary metabolites in *Solanum nigrum*, such as rutin nimbinene, meliacin and *quercertion*.

Conclusion

The microwave-assisted green synthesis was used to prepare SnO_2 nanoparticles. Compared to other methods, this method has several advantages. The crystallinity of the synthesized SnO_2 nanoparticles is excellent, and the nanoparticles have a higher surface area of 153 m^2/g. The spherical-shaped morphology was found for synthesized SnO_2 nanoparticles, and it was confirmed by HR-TEM. Biomolecules such as proteins and amino acids are thought to play a key role in the formation of SnO_2 nanoparticles using *Solanum nigrum* leaf extract. The photodegradation of EB dye with these synthesized nanoparticles is used to investigate photocatalytic behaviour. The photocatalytic degradation process is more efficient in the presence of sunlight irradiation due to the excitation of surface electrons. The high efficiency of SnO_2 nanoparticles as a photocatalyst makes them a promising candidate for dye degradation from industrial effluents. Additionally, the synthesized nanoparticles offer showed potent bacterial activities against both gram-positive and gram-negative micro-organisms. Overall, the results indicate that as-prepared SnO_2 nanoparticles are a suitable and attractive applicant for photocatalytic and antibacterial applications.

Data and materials availability Data of the manuscript will be made available on request.

Declarations

Competing interest The authors declare that there are no conflicts of interest.

Consent for publication Yes; all authors have full consents.

Ethics approval and consent to participate Not applicable.

References

1. Shafey ME (2020) Green synthesis of metal and metal oxide nanoparticles from plant leaf extracts and their applications: a review. Green Process Synth 9(1):304–339
2. Ovais M, Khalil A, Ayaz M, Ahmad I, Nethi S, Mukherjee S (2018) Biosynthesis of Metal nanoparticles via microbial enzymes: a mechanistic approach. Int J Mol Sci 19(12):4100
3. Zhu X, Pathakoti K, and Hwang HM (2019) Green synthesis of titanium dioxide and zinc oxide nanoparticles and their usage for antimicrobial applications and environmental remediation, Green synthesis, characterization and applications of nanoparticles, 223–263
4. Honarmand M, Golmohammadi M, Naeimi A (2019) Biosynthesis of tin oxide (SnO_2) nanoparticles using jujube fruit for photocatalytic degradation of organic dyes. Adv Powder Technol 30(8):1551–1557
5. Naseer M, Aslam U, Khalid B, Chen B (2020) Green route to synthesize zinc oxide nanoparticles using leaf extracts of *Cassia fistula* and *Melia azadarach* and their antibacterial potential. Sci Rep 10:1
6. Rodríguez-León E, Rodríguez-Vázquez BE, Martínez-Higuera A, Rodríguez-Beas C, Larios-Rodríguez E, Navarro RE, López-Esparza R, Iñiguez-Palomares RA (2019) Synthesis of gold nanoparticles using *Mimosa tenuiflora* extract, assessments of cytotoxicity, cellular uptake, and catalysis. Nanoscale Res Lett 14(1):1–16
7. Muthuvel A, Said NM, Jothibas M, Gurushankar K, Mohana V (2021) Microwave-assisted green synthesis of nanoscaled titanium oxide: photocatalyst, antibacterial and antioxidant properties. J Mater Sci: Mater Electron 32(8):23522–23539
8. Satheshkumar M, Anand B, Muthuvel A, Rajarajan M, Mohana V, Sundaramanickam A (2020) Enhanced photocatalytic dye degradation and antibacterial activity of biosynthesized ZnO-NPs using *curry leaves* extract with coconut water. Nanotechnol Environ Eng 5(3):1–11

9. Ghosh MK, Sahu S, Gupta I, Ghorai TK (2020) Green synthesis of copper nanoparticles from an extract of *Jatropha curcas* leaves: characterization, optical properties CT-DNA binding and photocatalytic activity. RSC Adv 10(37):22027–22035
10. Al-Zaqri N, Muthuvel A, Jothibas M, Alsalme A, Alharthi FA, Mohana V (2021) Biosynthesis of zirconium oxide nanoparticles using *Wrightia tinctoria* leaf extract: characterization, photocatalytic degradation and antibacterial activities. Inorg Chem Commun 127:108507
11. Kora AJ, Rastogi L (2018) Green synthesis of palladium nanoparticles using gum ghatti (*Anogeissus latifolia*) and its application as an antioxidant and catalyst. Arab J Chem 11(7):1097–1106
12. Timofeev VA, Mashanov VI, Nikiforov AI, Azarov IA, Loshkarev ID, Korolkov IV, Gavrilova TA, Yesin MY, Chetyrin IA (2020) Effect of annealing temperature on the morphology, structure, and optical properties of nanostructured SnO(x) films. Mater Res Express 7(1):015027
13. Matussin S, Harunsani MH, Tan AL, Khan MM (2020) Plant-extract-mediated SnO_2 nanoparticles: synthesis and applications. ACS Sustain Chem Eng 8(8):3040–3054
14. Karmaoui M, Jorge AB, McMillan PF, Aliev AE, Pullar RC, Labrincha JA, Tobaldi DM (2018) One-step synthesis, structure, and band gap properties of SnO_2 nanoparticles made by a low temperature nonaqueous sol-gel technique. ACS Omega 3(10):13227–13238
15. Akhir MAM, Rezan SA, Mohamed K, Arafat MM, Haseeb ASMA, Lee HL (2019) Synthesis of SnO_2 nanoparticles via hydrothermal method and their gas sensing applications for ethylene detection. Mater Today: Proc 17:810–819
16. Patil GE, Kajale DD, Gaikwad VB, Jain GH (2012) Preparation and characterization of SnO_2 nanoparticles by hydrothermal route. Int Nano Lett 2(1):1–5
17. Rashad MM, Ibrahim IA, Osama I, Shalan AE (2014) Distinction between SnO_2 nanoparticles synthesized using co-precipitation and solvothermal methods for the photovoltaic efficiency of dye-sensitized solar cells. Bull Mater Sci 37(4):903–909
18. Yu Z, Zhu S, Li Y, Liu Q, Feng C, Zhang D (2011) Synthesis of SnO_2 nanoparticles inside mesoporous carbon via a sonochemical method for highly reversible lithium batteries. Mater Lett 65(19–20):3072–3075
19. Barkley TK, Vastano JE, Applegate JR, Bakrania SD (2012) Combustion synthesis of Fe-incorporated sno_2nanoparticles using organometallic precursor combination. Adv Mater Sci Eng 1–8:2012
20. Krishnakumar T, Pinna N, Kumari KP, Perumal K, Jayaprakash R (2008) Microwave-assisted synthesis and characterization of tin oxide nanoparticles. Mater Lett 62(19):3437–3440
21. Mallikarjunaswamy C, Lakshmi Ranganatha V, RamuUdayabhanu R, Nagaraju G (2019) Facile microwave-assisted green synthesis of ZnO nanoparticles: application to photodegradation, antibacterial and antioxidant. J Mater Sci: Mater Electron 31(2):1004–1021
22. Krishnakumar T, Jayaprakash R, Pinna N, Singh VN, Mehta BR, Phani AR (2009) Microwave-assisted synthesis and characterization of flower shaped zinc oxide nanostructures. Mater Lett 63(2):242–245
23. Karthik K, Revathi V, Tatarchuk T (2018) Microwave-assisted green synthesis of SnO_2 nanoparticles and their optical and photocatalytic properties. Mol Cryst Liq Cryst 671(1):17–23
24. Singh J, Kaur H, Kukkar D, Mukamia VK, Kumar S, Rawat M (2019) Green synthesis of SnO_2 NPs for solar light induced photocatalytic applications. Mater Res Express 6(11):115007
25. Haritha E, Roopan SM, Madhavi G, Elango G, Al-Dhabi NA, Arasu MV (2016) Green chemical approach towards the synthesis of SnO_2 NPs in argument with photocatalytic degradation of diazo dye and its kinetic studies. J Photochem Photobiol, B 162:441–447
26. Bhosale TT, Shinde HM, Gavade NL, Babar SB, Gawade VV, Sabale SR, Kamble RJ, Shirke BS, Garadkar KM (2018) Biosynthesis of SnO_2 nanoparticles by aqueous leaf extract of *Calotropis gigantea* for photocatalytic applications. J Mater Sci: Mater Electron 29(8):6826–6834
27. Das J, Dhar SS (2020) Synthesis of SnO_2 quantum dots mediated by *Camellia sinensis* shoots for degradation of thiamethoxam. Toxicol Environ Chem 102(1–4):186–196
28. Wicaksono WP, Sahroni I, Saba AK, Rahman R, Fatimah I (2020) Biofabricated SnO2 nanoparticles using red spinach (*Amaranthus tricolor* L) extract and the study on photocatalytic and electrochemical sensing activity. Mater Res Express 7(7):075009
29. Vidhu VK, Philip D (2015) Biogenic synthesis of SnO_2 nanoparticles: Evaluation of antibacterial and antioxidant activities. Spectrochim Acta Part A Mol Biomol Spectrosc 134:372–379
30. Muthuvel A, Jothibas M, Manoharan C (2020) Effect of chemically synthesis compared to biosynthesized ZnO-NPs using *Solanum nigrum* leaf extract and their photocatalytic, antibacterial and in-vitro antioxidant activity. J Environ Chem Eng 8(2):103705
31. Muthuvel A, Jothibas M, Manoharan C (2020) Synthesis of copper oxide nanoparticles by chemical and biogenic methods: photocatalytic degradation and in vitro antioxidant activity. Nanotechnol Environ Eng 5(2):1–19
32. Muthuvel A, Jothibas M, Manoharan C, Jayakumar SJ (2020) Synthesis of CeO_2-NPs by chemical and biological methods and their photocatalytic, antibacterial and in vitro antioxidant activity. Res Chem Intermed 46(5):2705–2729
33. Kumar B, Smita K, Debut A, Cumbal L (2020) Synthesis and characterization of SnO_2 nanoparticles using cochineal dye. Appl Phys A 126(10):1–9
34. Gu F, Fen Wang S, Feng Song C, Kai Lü M, Xin Qi Y, Jun Zhou G, Xu D, Rong Yuan D (2003) Synthesis and luminescence properties of SnO2 nanoparticles. Chem Phys Lett 372(3–4):451–454
35. Xie W, Liang D, Li L, Qu S, Tao W (2019) Surface chemical properties and pore structure of the activated coke and their effects on the denitrification activity of selective catalytic reduction. Int J Coal Sci Technol 6(4):595–602
36. Viet PV, Thi CM, and Hieu LV (2016) The high photocatalytic activity of SnO_2 nanoparticles synthesized by hydrothermal method. J Nanomater. 1–8
37. Kim SP, Choi MY, Choi HC (2016) Photocatalytic activity of SnO_2 nanoparticles in methylene blue degradation. Mater Res Bull 74:85–89
38. Nasir Z, Shakir M, Wahab R, Shoeb M, Alam P, Khan RH, Mobin-Lutfullah M (2017) Co-precipitation synthesis and characterization of Co doped SnO_2 NPs, HSA interaction via various spectroscopic techniques and their antimicrobial and photocatalytic activities. Int J Biol Macromol 94:554–565
39. Sadeghzadeh-Attar A (2018) Efficient photocatalytic degradation of methylene blue dye by SnO_2 nanotubes synthesized at different calcination temperatures. Sol Energy Mater Sol Cells 183:16–24